

# Dynamics of Nonlinear Lattices

Christopher Chong and P.G. Kevrekidis

August 29, 2024

## Abstract

In this topical review we explore the dynamics of nonlinear lattices with a particular focus to Fermi-Pasta-Ulam-Tsingou type models that arise in the study of elastic media and, more specifically, granular crystals. We first revisit the workhorse of such lattices, namely traveling waves, both from a continuum, but also from a genuinely discrete perspective, both without and with a linear force component (induced by the so-called precompression). We then extend considerations to time-periodic states, examining dark breather structures in homogeneous crystals, as well as bright breathers in diatomic lattices. The last pattern that we consider extensively is the dispersive shock wave arising in the context of suitable Riemann (step) initial data. We show how the use of continuum (KdV) and discrete (Toda) integrable approximations can be used to get a first quantitative handle of the relevant waveforms. In all cases, theoretical analysis is accompanied by numerical computations and, where possible, by a recap and illustration of prototypical experimental results. We close the chapter by offering a number of ongoing and potential future directions and associated open problems in the field.

## 1 Introduction

The theme of nonlinear dynamical lattices is a very multifaceted one spanning a diverse range of disciplines within Mathematics, Physics and Engineering. Even if one restricts oneself to Hamiltonian or principally Hamiltonian lattices, the purview of an associated review effort is far too wide, given their diverse impact in different thematic areas. These extend from nonlinear optics, e.g., in the nonlinear dynamics of optical waveguides [1], to atomic Bose-Einstein condensates and the associated realm of optical lattices [2], and from models of the DNA double strand [3] to ones of electrical and mechanical elements [4]. The nonlinear waveforms that emerge in such systems, including traveling waves, kinks and breathers have, in turn, been summarized in various reviews [5, 6, 7] and books [8, 9, 10] (see also relevant chapters in [11, 12]). Dispersive shock waves are, arguably, less extensively treated in the discrete realm [13], although they have been widely popular in their continuum form in dispersive systems [14].

Within the confines of the present chapter, and given its specific parameters (including both its desired length, but also its target audience), we have thus opted to focus our attention on a particular example application and the associated developments over the past two decades, namely the theme of granular crystals [15, 16, 17, 18, 13]. One of the motivations for the relevant choice stems from the significant advances, including experimental ones, within this field that have enabled the realization of a wide palette of nonlinear excitations including the main workhorse of relevant studies in the form of the traveling wave [19, 16, 18], the subsequently experimentally accessed dispersive shock waves [13], but also the more recently proposed and realized discrete breathers [13], as well as extensions of these structures in heterogeneous [18] and higher-dimensional settings.

Another motivation for the choice of the granular crystals as a “paradigm of choice” for the illustration of the far-reaching impact of nonlinear dynamical lattices is its substantial potential as

a prototype for a wide range of concepts of interest to practical applications. For instance, such crystals have been proposed as a configuration that can enable the manifestation of the concept of “acoustic lenses” that may localize the energy in the form of “sound bullets” [20]. Another intriguing direction involves the use of such crystals (in the presence of defects) for the realization of acoustic switching and for inducing rectification in the work of [21, 22]. More recently, variants of such setups have been proposed for the implementation of acoustic gates and logic elements [23]. Yet another practical application has involved the use of granular crystal sensors (via the scattering of traveling waves) to assess whether bones are healthy or osteoporotic [24].

Our presentation of some of the principal ideas and nonlinear patterns of such metamaterial lattices will be structured as follows. In section 2, we will present an overview of the traveling waves in such systems. This will be followed by an exposition of the conditions under which time-periodic, exponentially-localized waveforms (so-called discrete breathers) can arise in 3. The more recent, somewhat more exotic and still rather elusive description of the dispersive shock waves will be explored in 4. We end the chapter summarizing and presenting a number of current and future directions in 5.

## 2 Traveling Waves

A seminal point towards the developments of interest to granular crystals (hereafter abbreviated as GCs) stemmed from the work of H. Hertz in 1881 [25] who characterized the force between two elastic bodies under what is now known as Hertz’s law:

$$F(\delta) = A[\delta]_+^{3/2}, \quad A = \frac{E\sqrt{2R}}{3(1-\nu^2)}, \quad (1)$$

Here,  $E$  stands for the elastic (Young’s) modulus and characterizes the material stiffness, while  $\nu$  represents the Poisson ratio, i.e., the tendency for transverse expansion under longitudinal compression;  $R$  stands for the body’s radius of curvature at contact. Here, we will mostly deal with spheres, hence it corresponds to the sphere’s radius. The  $+$  stands to indicate that the force is only active under contact (compression). The exponent  $3/2$ , i.e., the genuinely nonlinear character of the associated force is a principal source of the appeal of the relevant law towards the emergence of nonlinear excitations and for our considerations herein we will limit ourselves to that case. Yet, it is relevant to mention in passing that in other settings such as O-rings, cylindrical particles or hollow spheres the nature of the force may vary [26].

Now assembling a lattice of such spherical beads in the form of a GC (or a nonlinear mechanical metamaterial, as it is often referred to) leads to equations of motion encompassing the interaction of each bead with its nearest neighbors in the form of:

$$\ddot{u}_n = \frac{A_n}{M_n}[\delta_{0,n} + u_{n-1} - u_n]_+^p - \frac{A_{n+1}}{M_n}[\delta_{0,n+1} + u_n - u_{n+1}]_+^p. \quad (2)$$

Here,  $u_n$  stands for the displacement of the  $n$ -th particle of mass  $M_n$  (measured from the equilibrium). The so-called static precompression displacement (or simply precompression) is given by  $\delta_n = (F_0/A_n)^{1/p}$  and is associated with the (pre)compression force  $F_0$ . The expression for  $A_n$  is more complex for non-identical neighbors [15, 16],

$$A_n = \frac{4E_n E_{n+1} \sqrt{\frac{R_n R_{n+1}}{R_n + R_{n+1}}}}{3E_{n+1}(1-\nu_n^2) + 3E_n(1-\nu_{n+1}^2)}, \quad (3)$$

with the indices representing corresponding neighboring beads. Yet, here, for much of our discussion we will restrict considerations to homogeneous chains.

The strain formulation, where  $y_n = u_{n+1} - u_n$ , is also useful. In this case the original equation of motion Eq. (2) becomes:

$$\dot{y}_n = 2F(y_n) - F(y_{n-1}) + F(y_{n+1}) \quad (4)$$

where  $F(y) = [\delta_0 - y_n]_+^{3/2}$  and for simplicity we have assumed a time rescaling absorbing the factor of  $A/M$ .

When the precompression is finite, and indeed much larger than the pairwise relative displacements of the beads  $\delta_0 \gg |y_n|$ , it is straightforward to observe that the model Eq. (2) can be Taylor expanded and yields to leading order a discrete Laplacian, along with quadratic and subsequently cubic corrections similar to those emerging in the  $\alpha$  and  $\beta$ , respectively, installments of the famous Fermi-Pasta-Ulam model [27, 8, 28] that has been recently renamed to Fermi-Pasta-Ulam-Tsingou (FPUT) [29] to acknowledge contributions of Tsingou, a convention that we will use hereafter. In terms of the strain variable, the FPUT model is simply Eq. (4) with  $F(y) = K_2y + K_3y^2 + K_4y^3$ , where the  $K_j$  are coefficients, stemming, e.g., from a Taylor expansion. As such, it has been rigorously established that the model can be connected to (i.e., approximated by) the famous Korteweg-de Vries (KdV)

$$\partial_T Y + \partial_X^3 Y + Y \partial_X Y = 0. \quad (5)$$

using the ansatz  $y_n(t) = -\epsilon^2 \sigma^2 / (24K_3) Y(X, T)$ , where  $X = \epsilon(n - \sigma t)$ ,  $T = \sigma \epsilon^3 t / 24$  and where  $\sigma = \sqrt{Ap\delta_0^{p-1}/M}$  is the sonic speed limit for homogeneous chains. Then, the weakly supersonic waves of the FPUT (and accordingly of the GC) can be approximated by the continuum solitons of the KdV equation and indeed they inherit not only the existence properties, but also the stability properties of such waves [30, 31, 32]. This perspective has been leveraged to connect the GC traveling waves (TWs) with those of the KdV, including as regards the famous collision example of the tall and thin and fast soliton overtaking the short and fat and slow one [33]. Indeed, in this work, connections along the same vein were also forged with another famous integrable, yet genuinely discrete model, the Toda lattice. In terms of the strain, it is given by Eq. (4) with  $F(y) = e^y$ . The connection is made by simply matching the linear and quadratic Taylor coefficients of the granular chain and Toda lattice. The Toda reduction allows one to describe TWs and their interactions not only in the unidirectional case (as the KdV analysis allows), but also in the bidirectional setting of waves colliding when moving in opposite directions.

Our focus in this section will be primarily on the more mathematically interesting case where the precompression is absent, i.e.,  $\delta_0 = 0$ . For a considerable while, it was believed that this setting leads to, arguably, the most physically relevant example of a structure that was proposed in the 1990's in the context of nonlinear wave models devoid of linear dispersion (and, thus, featuring only nonlinear dispersion), the so-called compactons [34]. This belief stemmed from the attempt to produce a quasi-continuum model description of the underlying discrete system of Eq. (2). Absorbing the factor of  $A/M$  through a rescaling and using a(n artificially introduced) slow scale of space and time  $u_n(t) = U(X, T)$ , where  $X = \epsilon n$ ,  $T = \epsilon t$ , Nesterenko and collaborators obtained the long wavelength model of the form:

$$\partial_T^2 U = -\partial_X \left[ (-\partial_X U)^p + \frac{\epsilon^2}{12} \left( \partial_X^2 (-\partial_X U)^p - \frac{p(p-1)}{2} (-\partial_X U)^{p-2} \partial_X^2 U^2 \right) \right]. \quad (6)$$

One can also derive the corresponding equation for the strain defined as  $Y = \partial_X U$ . The key realization of Nesterenko and coworkers [15, 35] was that this PDE in the so-called co-traveling

frame associated with the variable  $\xi = X - cT$  can yield traveling waveforms as:

$$Y(X - cT) = c^m A \cos^m(B(X - cT)), \quad (7)$$

$$m = 2/(p - 1), \quad B = \sqrt{6(p - 1)^2/(p(p + 1))}. \quad (8)$$

Notice that these are periodic solutions, hence the proposed rubric for constructing the compactons, as is typically the case in such settings, is to isolate a period of this trigonometric solution and glue it with 0's on its two sides to construct such a pattern.

An alternative approach brought forth more recently [36] was to consider the strain variables already at the discrete level, see Eq. (4). Importantly, this is a Hamiltonian system whose Hamiltonian function can be written as:

$$H = \sum_{n \in \mathbb{Z}} \frac{1}{2} M_n \dot{u}_n^2 + V_n(u_{n+1} - u_n)$$

while the corresponding potential reads:

$$V_n(y_n) = \frac{2}{5} A_{n+1} [\delta_{0,n} - y_n]^{5/2} + \phi_n, \quad \phi_n = -\frac{2}{5} A_{n+1} [\delta_{0,n}]^{5/2} - A_{n+1} [\delta_{0,n}]^{3/2} y_n \quad (9)$$

It is notable that this approach is useful even in the presence of precompression because as observed in [37], it formulates the problem with a potential featuring  $V'_n(0) = 0$  and  $V''_n(0) \geq 0$ , thus enabling the use of the classic result of [38] towards a variational, yet rigorous proof of existence of a traveling wave.

The approach of [36] was to then retrieve a quasi-continuum model directly at the level of the strains (without passing from a quasi-continuum of displacements as before), in which case the resulting PDE reads:

$$\partial_T^2 Y = \partial_X^2 (Y^p) + \frac{\epsilon^2}{12} \partial_X^4 (Y^p). \quad (10)$$

Remarkably the latter features a compacton too:

$$Y(X - cT) = c^m A \cos^m(\tilde{B}(X - cT)), \quad (11)$$

$$m = 2/(p - 1), \quad \tilde{B} = \sqrt{3}(p - 1)/p. \quad (12)$$

Yet, equally remarkably, as is already evident by comparing Eq. (10) with Eq. (6), the two procedures [quasi-continuum limit derivation and strain variable transformation] do *not* commute, given the difference between the resulting equations and the associated compactons.

A natural question is which of the two functional waveforms is the “right” one in describing the actual traveling wave. While both of them are proximal to the TW, especially so for  $p = 3/2$ , the actual answer is, surprisingly, *neither*. Indeed, the relevant decay of the wave's tail is *doubly exponential* in nature. This was originally argued in [40], but was rigorously shown for this problem in the work of [41]. This was a byproduct of a reformulation of the relevant traveling wave problem (which is tantamount to an advance-delay differential equation) in Fourier space. The latter idea dates back to the work of [42]. More specifically, seeking a traveling wave in the form  $y_n(t) = \Phi(n - ct, t) = \Phi(\xi, t)$  yields the problem:

$$\partial_t^2 \Phi(\xi, t) = -c^2 \partial_\xi^2 \Phi(\xi, t) + 2c \partial_{\xi t} \Phi(\xi, t) + \left\{ (\Phi(\xi - 1, t))_+^{3/2} - 2(\Phi(\xi, t))_+^{3/2} + (\Phi(\xi + 1, t))_+^{3/2} \right\}, \quad (13)$$

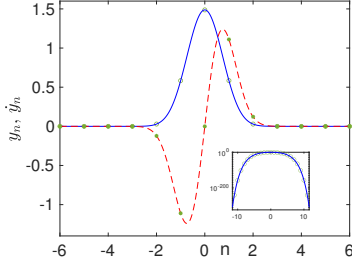


Figure 1: Traveling wave theoretical profile (blue solid) and its derivative (green dashed). The decay is shown in semilog in the inset. Lattice nodes denoted by the green points

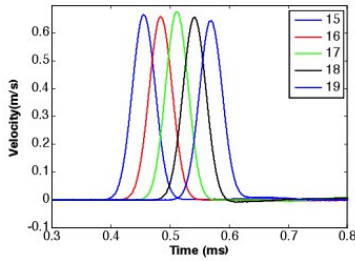


Figure 3: Experimental measurement of the velocity in adjacent nodes showcasing the traveling wave nature of the pulse in a granular crystal. Figure from Ref. [39]. Used with permission.

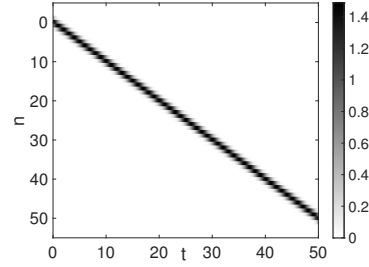


Figure 2: Space-time evolution of the exact traveling wave strain solution for a speed of  $c = 1$ .

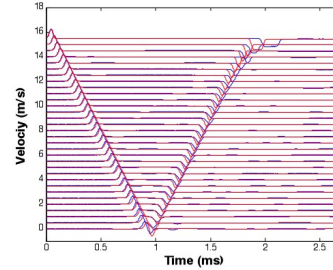


Figure 4: Collecting experimental measurements of the left panel into a space-time plot illustrating the traveling wave propagation along the granular crystal. Figure from Ref. [39]. Used with permission.

which, subsequently, for time-independent solutions in the co-traveling frame (i.e., only dependent on  $\xi$ ) and through the Fourier transform  $\phi(\xi) = \int_{-\infty}^{\infty} \hat{\phi}(k)e^{ik\xi} dk$  results in the fixed point scheme:

$$\hat{\phi}(k) = \frac{1}{c^2} \text{sinc}^2\left(\frac{k}{2}\right) \widehat{\phi^{3/2}}. \quad (14)$$

One can then Fourier transform back into real space to obtain the fixed point scheme in the real space variable in the form:

$$\phi(\xi) = \Lambda * \phi^{3/2} = \int_{-\infty}^{\infty} \Lambda(\xi - y) \phi^{3/2}(y) dy \quad (15)$$

The relevant kernel is  $\Lambda(\xi) = (1/c^2)[1 - |\xi|]_+$  and is referred to as the tent function. This formulation enables the numerically exact (up to a prescribed numerical accuracy) computation of the relevant waveform as is shown in Fig. 1-2 [intended to also contain a comparison between the numerical TW, and the two analytical ones of [15] and [36]]; this was illustrated since the early works of [42] in FPUT problems and more concretely for the granular problem in [41]. The latter work also showcased the decay of the strain pulse associated with the TW. Assuming  $c = 1$ , one can change to the variable  $z = \xi - y$  to rewrite Eq. (15) as:

$$\phi(\xi + 1) = \int_{-1}^1 \Lambda(z) \phi^{3/2}(\xi + 1 - z) dz \leq \phi^{3/2}(\xi) \Rightarrow \phi(\xi + n) \leq \phi(\xi)^{\left(\frac{3}{2}\right)^n}. \quad (16)$$

Here, the unit integral of the tent function has been used, as well as the positive, monotonically decreasing tail of the TW.

In the seminal works of pioneers in the field summarized, e.g., in [15] and [16] it was only possible to measure the speed of individual beads and to attempt to reconstruct, based on that, features such as the speed of the traveling wave. Yet, in recent times, remarkable experimental techniques such as Laser Doppler Vibrometry (LDV) have ushered the study of GCs into a new experimental era whereby it is possible to scope each bead within the configuration and use the Doppler effect to infer its speed as a function of time. A systematic repetition of the experiment and scoping of each bead enables the identification not only of the traveling nature of the structure by measuring some of the beads (see, e.g., Fig. 3), but also the visualization of the full evolution of the wave, as shown in Fig. 4.

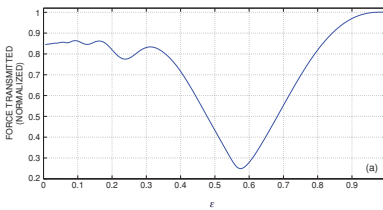


Figure 5: The numerical experiment showing the (normalized) response of a dimer chain, in terms of a transmitted force, as a function of the mass ratio  $\epsilon$ . Figure from Ref. [43]. Used with permission.

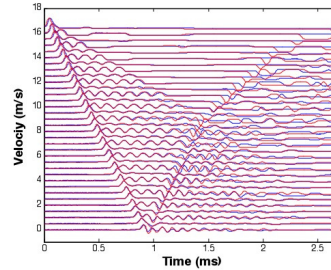


Figure 6: Space-time experimental evolution propagation associated with the case of  $\epsilon = 0.59$  showcasing the first and most dramatic resonance in a dimer chain Figure from Ref. [39]. Used with permission.

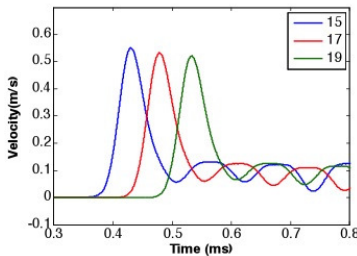


Figure 7: The evolution of the large mass beads of the top right panel case of  $\epsilon = 0.59$  as measured experimentally. Figure from Ref. [39]. Used with permission.

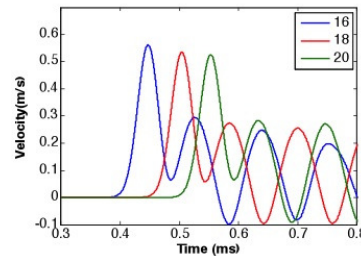


Figure 8: The evolution of the small mass beads of the top right panel case of  $\epsilon = 0.59$  as measured experimentally. Figure from Ref. [39]. Used with permission.

All of the above developments already introduced a mathematically, physically and experimentally challenging problem at the level of the monomer GC. Interestingly, however, the story gets far more complex once one considers heterogeneous chains. The study of such chains received considerable attention (including through experimental studies) in works after the mid-2000s; see, e.g., [44, 45]. These studies involved the prototypical realm of dimers (i.e., granular chains consisting of two types of beads, e.g., consisting of two different materials, or of the same material but different sizes), as well as trimers (3 different types of beads) or more complex heterogeneous chains of, e.g., 5:1 chains consisting of five beads of one type and then one of another. However, it

was not until the work [43] (see also the later one of [46]) that the truly fundamental alterations to the homogeneous, well-defined TW propagation were realized. This realization was subsequently extended to more complex chains in works such as those of [47, 48]. For a summary of the relevant findings, the interested reader is pointed to the authoritative description of [18].

Here we outline the most prototypical of these effects, namely the existence of so-called resonances and anti-resonances in dimer granular chains [43]. The originally proposed Gedankenexperiment was as follows: we know that in a GC, if we excite a bead on one end, in the absence of precompression, there are no sound waves, so the energy will be channeled into (typically) a TW which will be found to unobstructedly propagate throughout the lattice, as discussed above. What if we repeat this type of excitation in a dimer chain? The results were quite *dramatic*. It was found that if the ratio of the two masses within a dimer were 0.59, not only was the initial energy not going to be fully transmitted, but, in fact, only *less than 30%* of it would make it through. This is showcased quite strikingly in the experimental realization of the relevant setting that followed a few years later in the work of [39], showcased in the space-time strain evolution of Fig. 7. The theoretical transmission fractions predicted via numerical simulations can be seen (in comparison to the normalized monomer case of  $\epsilon = 1$  ( $\epsilon$  represents the ratio of the smaller to the larger mass)) in the panel of Fig. 5. It is clear in Fig. 6 that both the larger masses (whose speeds are represented in Fig. 7, as well as the more intensely vibrating smaller ones of Fig. 8 are shedding away energy as the wave passes through, leading eventually (as shown in Fig. 6) to the complete destruction of the wave. The latter is caused through the interference of the wave with the radiative tails it sheds. Entirely contrary to this resonance phenomenology is the case of  $\epsilon = 0.3428$ , the (2nd after that of the monomer) so-called anti-resonance whereby to every vibration of the larger mass correspond two vibrations of the smaller one leading to a(n essentially) perfect transmission and a genuine traveling wave being restored. The sequence of “quanta” of resonances and anti-resonances (in each of the latter, the smaller mass performs one additional vibration per one vibration of the large mass) was elucidated in the work of [43] (and subsequently considered in other settings in the works mentioned above) and was experimentally visualized in the work of [39]. In our view, it yields a remarkable illustration of how dramatically different the phenomenology of heterogeneous chains can be, in comparison to homogeneous ones. Moreover, these considerations initiated a considerable effort to understand the nature of waves in such diatomic lattices, e.g., of the Toda or of the FPUT type, from a more systematic mathematical perspective, respectively in works such as those of [49] and [50].

### 3 Discrete Breathers

A breather is defined as a structure that is periodic in time and localized in space. Breathers have a rich history, dating back to their first study in the context of the Sine-Gordon (sG) equation; see, e.g., [51, 11] for relevant reviews. Breathers in space-time continuous systems, such as the sG model, are somewhat special. While a breather’s frequency may lie in a frequency gap, coupling of higher order harmonics to the continuous spectrum of the system via nonlinearity is generally unavoidable since the linear passband extends to infinity. Such harmonic-coupling mechanisms to spatially extended plane waves will be detrimental to the spatial localization, and ultimately prevent the existence of genuine breather solutions. The sG model is an exception to this, and the coupling to higher order harmonics is only avoided due to the integrability of the equation. In contrast to spatially continuous systems, the passbands of spatially discrete systems are bounded from above, and thus such coupling mechanisms can controllably be avoided [52, 53]. Hence, the existence of breathers in discrete systems should be more generic. Indeed, the work of [54]

provided a mathematical foundation for this expectation illustrating that under (fairly generic) non-resonance conditions, discrete breathers should be expected to persist in a large class of nonlinear, spatially extended discrete dynamical systems. There has been a vast amount of research on discrete breathers, see for example [6].

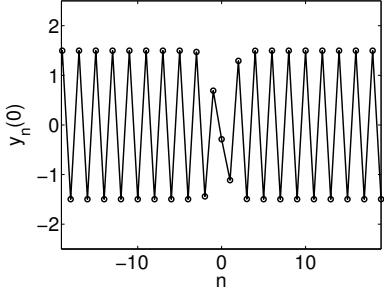


Figure 9: NLS approximation of a dark breather of the granular chain (markers). Solid lines are shown as a visual aid. The strain profile is shown. Figure from Ref. [55]. Used with permission.

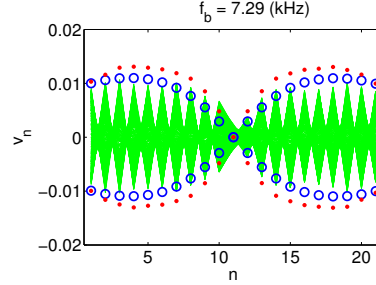


Figure 10: Experimental realization of a dark breather of the granular chain. Green line shows the time dynamics and the blue circles are the maxima/minima. The red dots correspond the model prediction. The velocity profile is shown. Figure from Ref. [56]. Used with permission.

In this section, we will focus on breathing structures of the granular chain. What we will see is that bright discrete breathers (i.e., ones on top of a vanishing background) are only possible in non-homogeneous granular chains. A related structure, called a dark-breather, can be found in homogeneous granular chains, which is where we start. We once again employ a multi-scale analysis, this time using the ansatz

$$y_n(t) = \epsilon Y(X, T) e^{i(kn + \omega t)} + \text{c.c.}, \quad (17)$$

where c.c. is the complex conjugate and the slow variables are  $X = \epsilon(n - ct)$  and  $T = \epsilon^2 t$ . This ansatz is similar to the one we used to derive the KdV equation, except now it includes a breathing in time (with frequency  $\omega$ ) and a spatial modulation with wavenumber  $k$ . The amplitude and slow time have also been suitably modified. Substituting Eq. (17) into Eq. (4) leads to a hierarchy of equations. At  $\mathcal{O}(\epsilon)$ , we retrieve the dispersion relation of the system, i.e.,  $\omega^2 = 4K_2 \sin^2(\frac{k}{2})$ . At the second order  $\mathcal{O}(\epsilon^2)$ , we are able to determine the group velocity  $c$  to be  $c = -\omega'(k)$ , where  $\omega' = \frac{d\omega}{dk}$ . Subsequently, at the cubic order  $\mathcal{O}(\epsilon^3)$ , the Nonlinear Schrödinger (NLS) equation is retrieved in the form:

$$i\partial_T Y(X, T) + \nu_2 \partial_X^2 Y(X, T) + \nu_3 Y(X, T) |Y(X, T)|^2 = 0. \quad (18)$$

See [57, 13] for the details of the full derivation. The coefficient of the dispersion reflects the (opposite of the) concavity of the dispersion relation, i.e.,  $\nu_2 = -\omega''(k)/2$ , while the nonlinearity coefficient is given by a considerably more elaborate expression. When the wavenumber is at the band edge ( $k = \pi$ ), it simplifies to  $\nu_3|_{k=\pi} = K_2^{-3/2}(3K_2K_4 - 4K_3^2) = B$ . At this wavenumber, the group velocity vanishes, and hence the breathers will be standing. At this same band edge, the concave down form of the dispersion relation gives  $\nu_2 > 0$ . However, for Taylor coefficients stemming from the granular chain, we have that  $B < 0$ , and hence we are in the realm of the so-called defocusing NLS equation [58] in which case one has the so-called dark soliton of the form,

$$Y(X, T) = \sqrt{\kappa/B} \tanh\left(\sqrt{\frac{-\kappa}{2\nu_2}}(X - X_0)\right) e^{i\kappa T}, \quad \kappa < 0, \quad (19)$$



Thus, the corresponding reconstruction of the solution with  $k = \pi$  of the original granular chain is of the form:

$$y_n(t) = 2\epsilon(-1)^n \sqrt{\frac{\kappa}{B}} \tanh\left(\sqrt{\frac{-\kappa}{2\nu_2}}\epsilon(n - x_0)\right) \cos(\omega_b t), \quad (20)$$

where  $\omega_b = \omega_0 + \kappa\epsilon^2$  is the breather frequency, with  $\omega_0 = \omega(\pi)$  being the linear cutoff frequency (in this case, the top of the acoustic branch of the dispersion relation). An example plot of this solution is shown in Fig. 9. Notice that the solution has a non-zero background, and has a density dip at the center of the lattice. This is the so-called dark breather, i.e., an exponentially localized, temporally periodic dark pattern (on top of a background), that additionally bears a staggered (alternating) form herein due to the  $k = \pi$  wavenumber.

Formula Eq. (20) provides an analytical approximation of the dark breathers of the granular chain that is accurate under the assumptions of which the formula was derived, namely with small amplitude, long wavelength, and with frequency close to the cutoff. To explore dark breathers beyond these assumptions, numerical computation is a useful tool.

We now provide a brief summary of how to compute time-periodic solutions in granular crystals, or lattices in general. More details can be found in [6]. We begin by writing Eq. (2) as a system of first order ODEs:

$$\dot{\mathbf{x}} = \mathbf{F}(t, \mathbf{u}, \mathbf{v}), \quad \mathbf{x} = \begin{pmatrix} \mathbf{u} \\ \mathbf{v} \end{pmatrix} \quad (21)$$

where  $\mathbf{u} = (u_1, \dots, u_p)^T$  and  $\mathbf{v} = \dot{\mathbf{u}}$ , respectively, represent the  $N$ -dimensional position and velocity vectors. In order to find periodic solutions to this system, we are searching for solutions  $\mathbf{x}$  so that  $\mathbf{x}(0) = \mathbf{x}(T)$  where  $T$  is the fixed period of the solution. This suggests that we define the Poincaré map:  $\mathcal{P}(\mathbf{x}^{(0)}) = \mathbf{x}^{(0)} - \mathbf{x}(T_b)$ , where  $\mathbf{x}^{(0)}$  is the initial condition and  $\mathbf{x}(T_b)$  is the result of integrating Eq. (21) forward in time until  $t = T_b$  using standard ODE integrators [59]. A periodic solution with period  $T$  (frequency  $1/T$ ) will be a root of  $\mathcal{P}$ . To obtain an approximation of this root, one can apply Newton's method [6, Sec. 3]. This method is generally robust in practice, if one is equipped with a suitable initial guess towards the waveform of interest, and has been employed for the computation of breathers, and other time-periodic solutions, in a number of settings, including Hamiltonian granular chains [60] and damped-driven ones [61]. An example dark-breather in a damped-driven granular chain found using the numerical procedure just described is shown in Fig. 10. This same figure also shows the experimental realization of a dark breather in a granular chain.

Another important consideration, especially if experiments are involved, is that of stability. For breathers, the theory is well understood see [6] and [7, 62]. Indeed, the linear stability problem is determined in the standard way: A small perturbation  $V(t)$  is added to a solution  $\mathbf{x}(t)$  that is time-periodic. The result  $\mathbf{x}(t) + V(t)$  is substituted into Eq. (21) to obtain an equation describing the evolution of  $V$ . Keeping only linear terms in  $V$  will lead to the so-called variational equations,

$$\dot{V} = [DF](t)V, \quad (22)$$

with initial data  $V(0) = \mathbf{I}$ ; and  $DF$  is the Jacobian of the equations of motion Eq. (21) evaluated at the point  $\mathbf{x}(t)$  (note that, when computing the Jacobian matrix for Newton's method, one needs to compute  $V(T)$ , so in some sense, Newton's method gives stability information "for free"). Since  $[DF](t)$  will be periodic in time with period  $T$ , Eq. (22) represents a Hill's equation. It is well known within Floquet theory [63], that the fundamental solutions of Eq. (22) have the property  $V(t + T) = \rho V(t)$ , where  $\rho$  is a so-called Floquet multiplier (FM). The Floquet multipliers are the eigenvalues of the matrix  $V(T)$ , where  $V(T)$  is the solution of Eq. (22) with initial data given by the identity matrix. Thus, the perturbation will exhibit exponential growth if there is at least

one FM with  $|\rho| > 1$ . In this case, the corresponding solution  $\mathbf{x}$  is deemed unstable. Otherwise, the solution is called spectrally stable. If the lattice is Hamiltonian, all FMs must lie on the unit circle for the solution to be spectrally stable, otherwise the solution is unstable, see [6, Sec. 4] for more details. One can connect such FMs with more familiar eigenvalue calculations via the correspondence  $\lambda = \log(\rho)/T$ , mapping instability to the real part  $\lambda_r > 0$ .

We have just described a set of powerful tools to study dark breathers of the granular chain. The tools themselves are not confined, of course, to dark breathers of the monomer granular chain. Indeed, let us explore some other relevant examples. If the coefficients  $\nu_2, B$  of Eq. (18) had the same signs then the corresponding NLS equation would be focusing, which has bright soliton solutions (i.e., solutions with a sech form). In that case, Eq. (17) would yield an approximate bright breather (here the terms bright simply emphasizes the fact the solution has tails going to zero). For any homogeneous chain, one cannot modify the concavity of the dispersion relation, and hence we must have  $\nu_2 > 0$ . The only way to change the sign of  $B$  is to have  $0 < p < 1$ , which corresponds to a so-called strain-softening lattice. Examples of such lattices include tensegrity [64], origami [65, 66], stainless steel cylinders separated by polymer foams [67], and hollow elliptical cylinders [68]. However, for granular chains, we have  $p = 3/2 > 1$ , which leads us to the conclusion that dark breathers are the only breather waveform possible in the homogeneous granular chain. The nonexistence of bright breathers in the FPUT lattice (and hence granular chain for small strains) result has been proved rigorously in [69] (using techniques different than multiple-scale analysis). Thus, to seek bright discrete breathers in the granular chain, we must move beyond homogeneous configurations.

If we consider a heterogeneous chain, we can alter the linear dispersion to our favor. In particular, dimer chains will feature an optical band in the dispersion relation in addition to the acoustic one found in homogeneous chains. Indeed, if one computes the dispersion relationship, one finds that the concavity of at the bottom of the optical band is opposite that of the top of the acoustic band. According to the previous NLS derivation, this would imply that  $\nu_2 < 0$  (and  $B < 0$  since  $p > 1$ ) and hence the NLS equation would be focusing. In this case the profile  $Y$  would take the form of a hyperbolic secant, and hence would be localized in space, i.e., it would represent a discrete bright breather. This heuristic argument can be verified by deriving the NLS equation from the dimer equations of motion directly, where one indeed finds a focusing NLS equation when choosing the wavenumber and frequency to be at the bottom of the optical band, see [70] for a detailed derivation. The numerical procedure to find breathers (and compute their stability) was used in [60, 61] for dimer lattices and for trimers [71], see Fig. 11 for an example. Experiments for dimers and trimers were reported on in [72] and [73], respectively. In [74] breathers in a lattice with alternating strain-softening and strain-hardening behavior was studied numerically and analytically. These findings clearly indicate how the presence of heterogeneity once again enables a complete modification of the monomer GC picture: just like for TWs, the presence of heterogeneity led to the complete destruction of perfectly propagating patterns (aside from isolated mass ratio “quanta”), similarly the dimer lattices enable an entirely new breed of breathers, namely bright breathers.

It is relevant to note here that while GCs have numerous advantages from an experimental standpoint (including their distributed visualization, their controllable heterogeneity and their controllable —based on precompression— nonlinearity), on-demand initialization is not one of them. Indeed, while the experimenters have considerable control over the boundary actuation of such systems, they do not generally have the ability to prescribe initial conditions at will. In that sense, the experimental realization of these breather initial conditions is not as straightforward of a task. This was bypassed in [56] through the destructive interference of two plane waves of suitable frequency in damped-driven GCs, leading to the spontaneous emergence of dark breathers. It was also sidetracked in dimer GCs in the work of [72] through the use of the nonlinear mechanism of

modulational instability, upon driving the chain at the unstable frequency of the optical band edge, which spontaneously was observed to lead to localization in the bandgap of the linear spectrum.

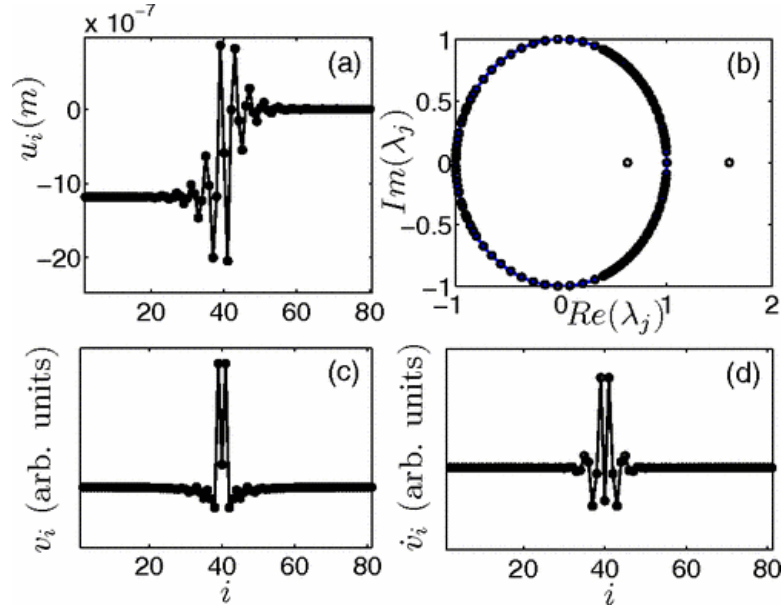


Figure 11: (a) Spatial profile (in displacement) of a breather of a dimer granular chain. (b) Corresponding locations of Floquet multipliers in the complex plane. We show the unit circle to guide the eye. Displacement (c) and velocity components (d) of the Floquet eigenvectors associated with the real instability. Figure from Ref. [75]. Used with permission.

Breathers cannot only be found in perfectly periodic lattices, like the monomer, dimer, and trimer ones just described, but also in defect lattices too. From the solid-state physics point of view, this is somewhat natural. When a waveform propagating in an otherwise perfect lattice encounters a defect, that defect particle will be excited and vibrate at the corresponding natural frequency. In terms of the linear theory, the defect will induce a linear mode that can possibly lie in the bandgap, e.g., if a defect mass is introduced that is lighter than the mass of the rest of the beads [76]. In the presence of nonlinearity, breathing structures can bifurcate from this linear defect mode, and can exist for an interval of frequencies within the gap. There has been a number of studies on defects and corresponding breathing modes in granular chains [77, 76, 75]. These showed also how to naturally interpolate between the defect limit and the dimer chain discussed above. Indeed, if there is a single defect mode [76, 75], a single defect mode exists (and a single family of bright breathers accordingly). If two defect beads are present, say two sites apart, then two defect breathing frequencies (and breather families) emerge [75, 77]. As the number of defect beads grows, so does the number of corresponding linear frequencies, until in the “infinite defect” limit, an entire (optical) band emerges, retrieving the above mentioned limit and its bright optical-band-derived breathers.

## 4 Dispersive Shock Waves

What happens to a medium or material when it is subjected to a sudden change of state? Such a question is important from an engineering perspective, with classic examples including explosions in shock tubes [78] or when gases or fluids are compressed in a piston chamber [79]. An idealization of

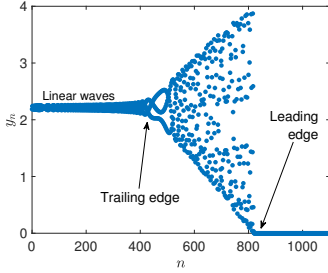


Figure 12: Upon initializing Eq. (4) with step-initial data, a DSW forms.

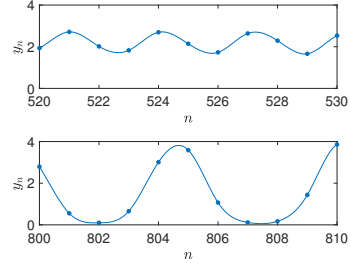


Figure 13: Two different zooms of solution shown in left panel (markers) and interpolating splines (lines). Each pattern appears to be described by a periodic wave, albeit with different wavelength, amplitude, and mean.

a sudden change of state in the context of nonlinear lattices is represented in the form of step-initial data, the so-called Riemann problem,

$$y_n(0) = \begin{cases} c, & n \leq 0 \\ 0, & n > 0 \end{cases} \quad \dot{y}_n = 0 \quad (23)$$

For fluid or gas dynamics based on space and time continuous conservation laws, such step initial data leads to the formation of fronts with infinite derivatives that travel through the medium at constant speed [80]. These are the classical shock waves. Let us see what happens when we initialize our example nonlinear lattice, Eq. (4), with step initial data with  $c = 4$ . The result is shown in Fig. 12. Rather than a front forming, it appears that an oscillating structure connecting states of different amplitude has formed. Evidently, the dispersive nature of Eq. (4) is responsible for the oscillations. For this reason, the structure shown in Fig. 12 is a so-called dispersive shock wave (DSW). Indeed, by inspection, its continuum approximation, see Eq. (10), the lattice equation can be viewed as a conservation law with higher order dispersive corrections (i.e., the terms pertaining to the higher powers of  $\epsilon$ ). The study of dispersive shock waves in one-dimensional (1D) nonlinear lattices (to be called lattice DSWs) dates back several decades ago [81], and continues to be an active area of study from the 1990s [82] and to this day [83, 84]. They have been explored numerically, and even experimentally in several works [15, 85, 86, 87, 88, 68]. Although much of the above motivation stems from the granular chains, it is of broader physical interest, as similar structures have been experimentally observed, e.g., in nonlinear optics of waveguide arrays [89]. It is important to also highlight in this context another setup that has recently emerged, namely tunable magnetic lattices [83]. Here, ultraslow shock waves can arise and can be experimentally imaged in terms of their space-time evolution.

To get a sense of how one could analyze a DSW, let us inspect the solution more closely. Figure. 13 shows a zoom of the DSW near the trailing edge (i.e., the back part of the DSW, see the label in Figure. 12) and near the leading edge (i.e., the front part). At this microscopic level, the solution appears to be a periodic wave, however the parameters, such as the mean, amplitude, and wavenumber, seem to depend on “where” in the lattice one looks. This suggests that the DSW is actually described by a single periodic wave,  $\Phi(n - ct)$ , whose mean, wavenumber, and amplitude vary slowly across its domain. This is the idea behind modulation theory, pioneered by Whitham over 50 years ago [90]. Modulation equations describing the periodic wave parameters can be derived using, e.g., the method of the so-called averaged Lagrangian [90]. Equivalent alternative approaches

also exist with, arguably perhaps, the most accessible among them pertaining to the averaging of the conservation laws of the model of interest [14]. Such approaches have been successfully employed to study DSWs in several space-time continuous models, as summarized in [91, 92, 14]. For lattices, however, this approach leads to modulation equations that are quite cumbersome [93, 94]. A principal reason for this feature can be thought as the fact that the periodic wave  $\Phi$  satisfies an advance-delay equation (the one we encountered in Eq. (13)), in which case there is no closed-form solution. An additional significant complication stems from the potential absence in the context of lattices of the feature of a momentum conservation law. While this is not the case in the FPUT lattices of interest herein, in general, the lack of integrability (and, more practically, of a sufficient number of the “first few” conservation laws) poses a significant hurdle to Whitham theory considerations herein. In such situations, one will often resort to other approximations, by, e.g., focusing on the trailing or leading edge dynamics [95], employing a harmonic approximation for the periodic waves [96], or using a data-driven approach to reduce the dynamics to a planar ODE [97]. In this chapter, we will focus on two integrable limits, in which case tractable analytical approximations can be obtained, and hence could be useful for practical engineering applications.

We start with the simplest integrable limit, the KdV equation, see Eq. (5). Solutions of this KdV equation that are of critical importance for our purposes are the periodic traveling waves,

$$Y(X, T) = r_1 + r_2 - r_3 + 2(r_3 - r_1) \operatorname{dn}^2 \left( \sqrt{\frac{r_3 - r_1}{6}} (X - VT); m \right), \quad (24)$$

where  $V = \frac{r_1 + r_2 + r_3}{3}$ ,  $m = \frac{r_2 - r_1}{r_3 - r_1}$  and  $\operatorname{dn}$  is one of the Jacobi elliptic functions with elliptic parameter  $0 \leq m \leq 1$  [98]. Note that these waves are parameterized by  $r_1, r_2, r_3$ . Assuming the parameters of the periodic wave (i.e., the  $r_j$ 's) vary slowly with respect to  $X, T$  and averaging three of the conserved quantities of the KdV equation over a period yields a set of three Whitham modulation equations [90]. In the case of self-similar solutions,  $r_j = r_j(X/T)$ , these equations have the form  $(S_j - X/T)r'(X/T) = 0$ , where the characteristic speeds  $S_j$  are nonlinear functions of  $r_1, r_2$  and  $r_3$ . Thus, in this self-similar framework,  $r_j$  is either constant or  $X/T$  is equivalent to the characteristic speed  $S_j$ . If one assumes the following initial data for the KdV equation

$$Y(X, 0) = \begin{cases} 1, & X < 0 \\ 0, & X > 0 \end{cases} \quad (25)$$

then one finds

$$r_1 = 0, \quad r_2 = m, \quad r_3 = 1.$$

Details for the derivation of these expressions can be found in [99, 100, 14]. Substituting these expressions into Eq. (24), and returning to the granular variables in the strain  $y_n(t)$ , we obtain the following approximation for the core of the granular chain DSW:

$$y_n(t) = -c \frac{\sigma^2}{K_3} \left( 2 \operatorname{dn}^2 \left( \sqrt{4c} \left( n - \left( 1 + \frac{m+1}{3} c \right) \sigma t + \Theta_0(n, t) \right); m \right) - (1 - m) \right) \quad (26)$$

where  $c = \epsilon^2/24$  is a small parameter,  $\sigma$  is the sound speed and the variables  $n, t$  are parameterized by  $m$  through the expression

$$\frac{(n - \sigma t)}{\sigma c t} = S(m), \quad (27)$$

with  $S(m)$  given by

$$S(m) = \frac{1+m}{3} - \frac{2}{3} \frac{m(1-m)K(m)}{E(m) - (1-m)K(m)}, \quad (28)$$

where  $K(m)$  and  $E(m)$  are complete elliptic integrals of the first and second kind, respectively. Note Eq. (26) contains a slowly modulated phase shift  $\Theta_0(n, t)$  that is not accounted for by the leading order Whitham theory [101]. We have included it here, as it will be treated as a fitting parameter to account for a phase mismatch between theory and simulation.

From the above expression we can write the trailing edge speed ( $n/t = s_-^{\text{KdV}}$ ) and leading edge speed ( $n/t = s_+^{\text{KdV}}$ ) in terms of the original granular chain variables,

$$s_-^{\text{KdV}} = \sigma(1 - c) \quad (29a)$$

$$s_+^{\text{KdV}} = \sigma \left( 1 + \frac{2}{3}c \right). \quad (29b)$$

Thus the leading edge speed is supersonic, as it necessarily lies above the sound speed  $\sigma$ , whereas the trailing edge speed is subsonic. Since the parameter  $\epsilon$  is assumed to be small (and hence so is  $c$ ), the leading edge is traveling just above the sound speed, and the trailing edge is slightly below.

This formulation gives a way to approximate the DSW resulting from step initial data in the strain, given in Eq. (4); see [84] for comparisons to numerical simulations. However, these initial conditions imply the entire strain profile must be specified, which is generally hard to achieve in GC experiments, as discussed above. The more relevant initial condition for the granular chain, and other similar lattices, is a collision at one side of the chain. In [87] it was shown that such a collision is well approximated by a continuous velocity applied to the end of a semi-infinite chain (this is the so-called piston problem [79]). By an appropriate change of variables, the piston-problem initial conditions are equivalent to an infinite chain with a velocity shock [93], namely,

$$u_n(0) = 0 \quad (30a)$$

$$\dot{u}_n(0) = -2c \text{sign}(n) \quad (30b)$$

where  $\text{sign}(0) = 0$ . Notice that this initial condition is given in terms of the displacement variable  $u_n$ . Nonetheless, we continue to report results in terms of the strain  $y_n = u_n - u_{n+1}$  for consistency. With such an initial condition, it is reasonable to suppose, based on the linear theory [102], that the trailing edge (in the strain) will have a mean close to  $2c$ . This suggests that the  $c$  defined assuming the initial data Eq. (23) is the same as the  $c$  defined in Eq. (30). Indeed, this was the motivation for defining  $c = \epsilon^2/24$  previously. This means we can apply the prediction Eq. (26), even when the initial condition is given by a velocity shock. Fig. 14 shows a comparison of a DSW formed given a velocity shock (markers) and the KdV prediction for  $c = 0.1$ . The microscopic time  $t$  is chosen such that macroscopic time  $T_f = 1200$  is fixed. Figure 15 shows the same simulation data, but now with windowing such that the microscopic variables  $(n, t)$  are fixed. In particular, intensity plots of the strain are shown. The prediction of the leading and trailing speed from the KdV equation are shown as solid black lines.

We now turn our attention to a different analytical approximation of the granular chain DSW, namely, one based on the Toda lattice, see discussion in Sec. 2. There is a four parameter family of traveling periodic waves of the Toda lattice, parameterized by  $E_1, E_2, E_3, E_4$ . In terms of the strain, the formula is,

$$y_n(t) = \log \left( 2\hat{R}_n(t) + \frac{1}{2}(E_1^2 + E_2^2 + E_3^2 + E_4^2) - \mu_n^2(t) - b_n^2(t) \right) \quad (31)$$

where

$$b_n(t) = E_1 + E_2 + E_3 + E_4 - 2\mu_n(t) \quad (32)$$

and

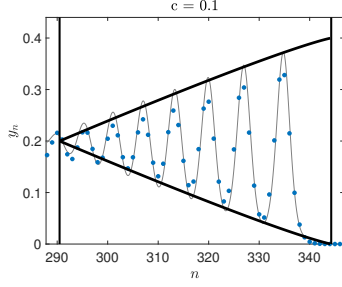


Figure 14: Granular chain simulations with an initial velocity shock compared to the KdV prediction with  $c = 0.1$ . Figure from Ref. [97]. Used with permission.

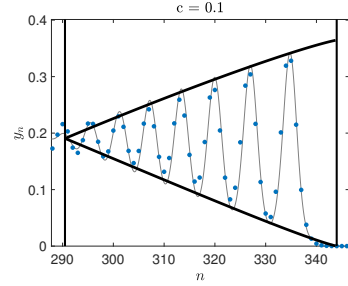


Figure 15: Same as 14 but the simulation is compared to the Toda approximation. Figure from Ref. [97]. Used with permission.

$$\begin{aligned}
\mu_n(t) &= E_2 \frac{1 - (E_1/E_2) B \operatorname{sn}^2(Z_n(t), m)}{1 - B \operatorname{sn}^2(Z_n(t), m)}, \\
Z_n(t) &= 2nF(\Delta, m) + \omega t + Z_0, \\
m &= \frac{(E_3 - E_2)(E_4 - E_1)}{(E_4 - E_2)(E_3 - E_1)}, \\
\hat{R}_n(t) &= -\sigma_n(t) \sqrt{P(\mu_n(t))} \\
P(z) &= (z - E_1)(z - E_2)(z - E_3)(z - E_4), \\
\omega &= \sqrt{(E_4 - E_2)(E_3 - E_1)} \\
\Delta &= \sqrt{\frac{E_4 - E_2}{E_4 - E_1}}, \quad B = \frac{E_3 - E_2}{E_3 - E_1}.
\end{aligned}$$

In the above equations,  $\operatorname{sn}(z, m)$  is the Jacobi elliptic sine,  $F(z, m)$  is the inverse of  $\operatorname{sn}(z, m)$ ,  $Z_0$  is an arbitrary translation parameter (phase),  $\mu_n(t)$  is the Dirichlet eigenvalue of the scattering problem for the Toda lattice and  $\sigma_n(t) = \pm 1$  is the sign associated with  $\mu_n(t)$ , and determines whether  $\mu_n(t)$  is increasing or decreasing as a function of  $n$  and  $t$ . For numerical computations, we used  $\sigma_n(t) = -\operatorname{sign}(\operatorname{mod}(Z_n(t)/K_m) - 1/2)$ . Notice how the Toda traveling wave solution is more complicated than its KdV counterpart in Eq. (24). So while we may anticipate a better approximation (since no long-wavelength assumption is made), the tradeoff is a formula that will be considerably more cumbersome.

Like in the KdV case, one can derive a system of modulation equations (4 in the Toda case) that can be written in diagonalized form, and solved in the self-similar frame  $E_j = E_j(n/t)$  assuming an initial velocity shock. Three of the parameters are constant in the self-similar frame, and one depends on the parameter  $m$  [103, 104]. In particular,

$$E_1 = -(1 + c), \quad E_2 = -(c - 1), \quad E_3(m) = (c + 1) \frac{1 - c(1 - m)}{1 + c(1 - m)}, \quad E_4 = (c + 1). \quad (33)$$

Assuming  $0 < c < 1$ , the core of the DSW is described by Eq. (31) with parameters given via Eq. (33) where  $n, t$  are parameterized by  $m$  through the expression

$$\frac{c(c + 1)}{1 + c(1 - m)} \frac{(1 + c(1 - m))E(m) - (c + 1)(1 - m)K(m)}{(c + 1)K(m) - (1 + c(1 - m))\Pi\left(\frac{cm}{c+1} \middle| m\right)} =: s^{\text{Toda}}(m) = \frac{n}{t} \quad (34)$$

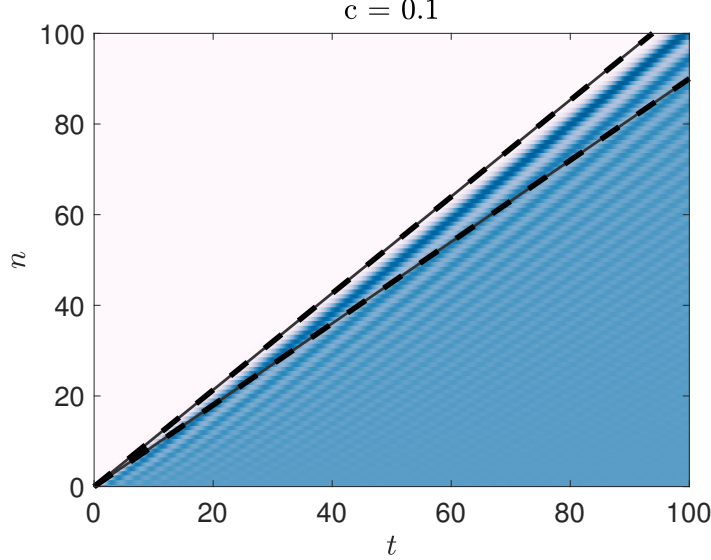


Figure 16: Intensity plot of the granular chain simulation with an initial velocity shock, Eq. (30). The solid lines are the estimates of the leading and trailing edge from the KdV description, and the dashed lines are from the Toda description. The small parameter is  $c = 0.1$ . Figure from Ref. [97]. Used with permission.

where  $K(m)$ ,  $E(m)$  and  $\Pi(n|m)$  are complete elliptic integrals of the first, second, and third kind respectively, and  $s^{\text{Toda}}(m)$  is the third characteristic velocity of the Whitham equations for the Toda system. As before,  $m \rightarrow 0$  corresponds to the trailing, harmonic wave edge (recall  $0 < c < 1$ ) and  $m \rightarrow 1$  corresponding to the leading, solitary wave edge. The trailing edge speed ( $s_-^{\text{Toda}}$ ) and leading edge speed ( $s_+^{\text{Toda}}$ ) are obtained as limiting values in Eq. (34), in particular

$$\lim_{m \rightarrow 0} s^{\text{Toda}}(m) = s_-^{\text{Toda}} = 1 - c, \quad \lim_{m \rightarrow 1} s^{\text{Toda}}(m) = s_+^{\text{Toda}} = \frac{\sqrt{c(c+1)}}{\log(\sqrt{c} + \sqrt{c+1})} \quad (35)$$

Once again, we have that the leading edge speed is supersonic whereas the trailing edge speed is subsonic. We can also compute the trailing edge mean and leading edge amplitude from Eq. (31),

$$\bar{y}_-^{\text{Toda}} = 2 \log(1 + c), \quad a_+^{\text{Toda}} = 2 \log(1 + 2c) \quad (36)$$

Notice that trailing edge speed predictions from Toda and KdV are identical, namely  $s_-^{\text{Toda}} = s_-^{\text{KdV}}$ . Indeed, the remaining three edge characteristics are also related. By Taylor expanding the remaining formulas in Eqs. (35) and (36) about  $c = 0$  shows that the leading order behavior is identical to the KdV approximation. Namely, for small  $c$  we have that

$$s_+^{\text{Toda}} \approx 1 + \frac{2}{3}c = s_+^{\text{KdV}}, \quad \bar{y}_-^{\text{Toda}} \approx 2c = \bar{y}_-^{\text{KdV}}, \quad a_+^{\text{Toda}} \approx 4c = a_+^{\text{KdV}} \quad (37)$$

Thus, to leading order, both the KdV and Toda limits yield the same approximation of the edge characteristics.

It is important once again to put these results in the proper context in the setting of GCs. What we have done herein is that we have leveraged a mapping through multiple scales (in the KdV case) or a matching (up to the maximal allowable order) in the Toda case of the GC problem *with*



*precompression* to well-established integrable analogs for which the rich structure of integrability (the periodic solutions, the conservation laws, the Lagrangian/Hamiltonian structure, the Riemann invariants, etc.) enable the completion of the Whitham equation “program” and therefore the approximate, yet quite satisfactory description of the GC DSWs. On the other hand, we have not addressed the much more complex case of the so-called sonic vacuum, i.e., when the precompression  $\delta_0 = 0$ . Yet, it was in the latter limit that the principal earlier studies [86, 88, 87] were conducted. Naturally, this raises the question of how to address the latter limit. It turns out that some of the asymptotic techniques for describing the trailing and leading edges of DSWs, such as [95], can be carried out in discrete as well as continuous systems and can be brought to bear in the GC without precompression. Yet, in order to perform a systematic analysis of both limits and to obtain a framework for Whitham modulation theory a quasi-continuum methodology can be proposed. While those of [15] and [36] suffer from issues of well-posedness, regularized variants thereof in the spirit of Rosenau’s work [105, 106] bypass this concern and are promising grounds for developing a sonic-vacuum DSW description. This is an interesting direction of ongoing work [107].

## 5 Summary and Future Directions

In this chapter we summarized some of the key tools to study nonlinear lattices. We used the granular chain as the vehicle of choice, formulating the mathematical equation framework (of FPUT systems) in order to demonstrate how these tools, such as continuum modeling, Fourier analysis, and various numerical methods could be applied. Along this short journey, we sought to highlight some of the main results concerning granular chains revolving around three fundamental structures, namely the solitary waves, the breathers, and the dispersive shock waves. In this section, we touch upon some emerging directions in the realm of nonlinear lattices.

While the granular chain serves as a canonical example of a nonlinear lattice, there exists a variety of other platforms that can be modeled in the general framework of (2) upon modifying existing, or adding additional, terms. We have already discussed periodic arrangements and defect lattices, but there exist also systems incorporating disorder, where effects such as Anderson localization are possible [108], and superdiffusive transport has been realized [109]. Additionally, systems with an onsite force have also been explored. Such examples include the study of breathers in the Newton’s cradle [110] and also the exploration of [111, 112]. Traveling waves as well as nanoptera (waves with small amplitude tails) were predicted in dimers [113, 49], as well as in locally resonant systems [114, 115] (in the latter, in the setting of the so-called woodpile chains, they were also observed [116]); see also the recent review [117]. One can also consider the intersite force function to be of a slightly more general form, namely  $F(x) = A(d + \text{sign}(p)x)^p$ . The case of  $0 < p < 1$  corresponds to a so-called strain-softening lattice. In such lattices, traveling waves have been studied in the context of tensegrity [64], origami chains [65, 66] and stainless steel cylinders separated by polymer foams [67], whereas dispersive shock waves have been explored in hollow elliptical cylinders [68]. Breathers in lattices that alternate between softening and hardening were explored recently in [74]. An array of repelling magnets corresponds to the case with  $p < 0$ , in which case traveling waves [118], and breathers in one [119] and two dimensions [120] have been studied, as well as DSWs [83]. Magnetic lattices with time-modulated stiffness properties, falling into the class of so-called phononic time crystals, have also been studied, where e.g., time-periodic and wavenumber bandgap breathers have been explored [121, 122].

Magnetic lattices constitute a particularly interesting example, as they also include long-range interactions, whereby each neighbor is coupled to all other neighbors, albeit weakly. In [119], breathers with algebraically decaying tails in lattices with long-range interactions were shown to

exist, confirming theoretical predictions from decades prior in [123]. The notion of long-range media is intimately connected to that of fractional media. Fractional media, where the underlying model equations have the usual (integer) derivatives replaced with fractional ones (based on suitable integral definitions), are relevant in many areas, such as fluid and quantum mechanics, and more [124]. In the latter book, connections have been made to fractional discrete variants of the nonlinear Schrödinger and sine-Gordon equations, suggesting that a near-future analogue will be FPUT lattices, that, in turn, will be connected with fractional KdV continuum models (also studied therein). Fractional media in nonlinear lattices, such as electrical ones and those of the DNLS type have also been recently proposed [125], where the the fractional derivatives tend to, among other effects, be tantamount to long-range interactions which can accordingly, e.g., decrease the threshold for the self-trapping transitions, induce bistability, etc. We expect this to be a direction that is further explored in future studies; it also remains to be seen whether, in addition to spatial fractional derivatives, temporal fractional derivatives such as the Caputo derivative for wave-like systems may be of practical interest (in addition to being of mathematical one) [126].

Band topology, an inherently linear phenomenon, has been explored in electronic materials, optical lattices in cold-atom systems, and topological photonics where the behavior in the presence of corners, edges, and surfaces has been explored [127, 128]. The ability of the relevant topological systems to preserve features under continuous deformation presents exceptional promise for guiding of wave propagation [129], while demonstrating robustness against various imperfections. It is for that reason that relevant applications have recently extended to both acoustics [130, 131], and mechanics [132, 131]. While important steps have been made as concerns the interplay of nonlinearity and novel linear states (such as the topological ones just mentioned) in lattices, e.g., in the context of optical waveguides, as summarized in the recent review of [133], we expect this direction to be one warranting significant additional progress in the near future.

Another exotic linear phenomenon concerns the presence of the so-called flat bands, which arise as completely degenerate energy bands in certain tight-binding lattices with macroscopic degeneracy [134, 135]. This phenomenon has significant implications such as the associated vanishing group velocity, which, in turn, suppresses transmission, while the system produces (generically, as it can be proved) compactly supported localized (linear) states. These can be indeed localized with a strictly finite support. The particular sensitivity of such bands to perturbation effects enables a wide range of intriguing features including localization-delocalization transitions, symmetry-breakings, compact nonlinear breathing or localized states, ferromagnetic and superfluid-like features among others. Once again, the versatility of dispersive platforms has enabled the realization of such states in photonic, polaritonic, electrical, magnonic and even phononic 2D [136] and acoustic 3D [137] systems. Once again, the interplay of this key linear feature with nonlinearity is far less explored; one recent experimental example is in the electrical lattice realm of [138], where nonlinear compactly supported breathing states for diamond and stub lattices were realized. Further exploration of the fascinating features of Kagomé [139], Lieb lattices [140, 141] and other similar settings [142] is certainly worthwhile as well.

Most of the considerations listed above are in the realm of one-dimensional lattices, and indeed the vast majority of studies have been in this setting. The effect of dimensionality can be significant, however. For example, in square or hexagonal lattices, a single particle is in contact with multiple particles. Thus, if energy is applied to a single particle, it will be distributed to an expanding array of neighbors [143]. This spreading of energy should prevent the possibility of genuine 2D traveling solitary waves in such lattices. There have been, however, several studies related to the notion of traveling waves. These include those focusing on the dynamics after impacts, networks of 1D chains that live in 3D space, and “sound bullets” which are waves that can be guided to (focus on) preselected lattice sites within the crystal. Such findings are summarized in [13]. While the

geometry of the higher dimensional lattices seems to prohibit genuine traveling solitary waves, it still affords the possibility of breathers. Indeed, they have been studied in hexagonally arranged magnetic and other related lattices, see [120] and references therein. Dispersive shock waves in 2D lattices should also be possible, however they remain rather unexplored. Furthermore, it is in such higher dimensional settings where the effect and robustness of topological modes could prove especially versatile; while important steps have been made in this direction [144], numerous further insights promise to arise along this vein.

Finally, modern computational approaches involving data driven methods have just started to make an impact on field of nonlinear waves. For example, recently in [145, 146] topological states in elastic media were explored through the lens of dynamic mode decomposition, which is a dimensionality reduction method to create reduced-order models which identifies spatiotemporal coherent structures from high-dimensional data [147]. While such methods have been applied to a host of other scientific fields such as fluid dynamics, control, robotics, and biological science [145] their application in the realm of nonlinear lattices remains in its infancy and thus serves as a crucial future direction in the field. Moreover, the identification and modeling of features that have long remained controversial (such as the inclusion of dissipation; see the discussion of [13, 148]) could benefit from the emerging boom of data-driven physics-informed, sparse identification techniques such as PINNs [149], SINDy [150], deepXDE [151] (see also the review of [152]). Such techniques are only starting to be used to discover mathematical and potentially physically-interpretable-features from data in nonlinear dynamical lattices (see, e.g., [153] for a recent example) and progress in this direction will, undoubtedly (in our view), significantly impact future discoveries in nonlinear lattice dynamics.

## References

- [1] Falk Lederer, George I. Stegeman, Demetri N. Christodoulides, Gaetano Assanto, Moti Segev, and Yaron Silberberg. Discrete solitons in optics. *Physics Reports*, 463(1):1–126, 2008.
- [2] Oliver Morsch and Markus Oberthaler. Dynamics of bose-einstein condensates in optical lattices. *Rev. Mod. Phys.*, 78:179–215, Feb 2006.
- [3] M. Peyrard. Nonlinear dynamics and statistical physics of DNA. *Nonlinearity*, 17:R1, 2004.
- [4] M. Remoissenet. *Waves Called Solitons*. Springer-Verlag, Berlin, 1999.
- [5] S. Flach and C.R. Willis. Discrete breathers. *Physics Reports*, 295(5):181–264, 1998.
- [6] Sergej Flach and Andrey V. Gorbach. Discrete breathers — Advances in theory and applications. *Physics Reports*, 467(1-3):1–116, oct 2008.
- [7] S. Aubry. Discrete breathers: Localization and transfer of energy in discrete Hamiltonian nonlinear systems. *Physica D*, 216:1, 2006.
- [8] G. Gallavotti. *The Fermi–Pasta–Ulam Problem: A Status Report*. Springer-Verlag, Berlin, Germany, 2008.
- [9] P.G. Kevrekidis. *The discrete nonlinear Schrödinger Equation*. Springer-Verlag, Heidelberg, 1st edition, 2009.
- [10] D. Pelinovsky. *Localization in Periodic Potentials: From Schrödinger Operators to the Gross–Pitaevskii Equation*. Cambridge University Press, Cambridge, 2011.

- [11] J. Cuevas, P.G. Kevrekidis, and F.L. Williams. *The sine-Gordon Model and its Applications: From Pendula and Josephson Junctions to Gravity and High Energy Physics*. Springer-Verlag, Heidelberg, 2014.
- [12] J. Cuevas-Maraver and P.G. Kevrekidis (eds.). *A dynamical perspective on the  $\phi^4$  model*. Nonlinear Systems and Complexity. Springer International Publishing, 1st edition, 2019.
- [13] C. Chong and P. G. Kevrekidis. *Coherent Structures in Granular Crystals: From Experiment and Modelling to Computation and Mathematical Analysis*. Springer, New York, 2018.
- [14] G.A. El and M.A. Hofer. Dispersive shock waves and modulation theory. *Physica D: Nonlinear Phenomena*, 333:11, 2016.
- [15] V.F. Nesterenko. *Dynamics of Heterogeneous Materials*. Springer-Verlag, New York, 2001.
- [16] S. Sen, J. Hong, J. Bang, E. Avalos, and R. Doney. Solitary waves in the granular chain. *Phys. Rep.*, 462:21, 2008.
- [17] A. F. Vakakis. Analytical methodologies for nonlinear periodic media. In *Wave Propagation in Linear and Nonlinear Periodic Media (International Center for Mechanical Sciences (CISM) Courses and Lectures)*, page 257. Springer-Verlag, Berlin, Germany, 2012.
- [18] Yu. Starosvetsky, K.R. Jayaprakash, M. Arif Hasan, and A.F. Vakakis. *Dynamics and Acoustics of Ordered Granular Media*. World Scientific, Singapore, 2017.
- [19] S. Y. Wang and V. F. Nesterenko. Attenuation of short strongly nonlinear stress pulses in dissipative granular chains. *Phys. Rev. E*, 91:062211, 2015.
- [20] A. Spadoni and C. Daraio. Generation and control of sound bullets with a nonlinear acoustic lens. *Proc. Natl. Acad. Sci. USA*, 107:7230, 2010.
- [21] N. Boechler, G. Theocharis, and C. Daraio. Bifurcation-based acoustic switching and rectification. *Nat. Mater.*, 10(9):665–668, 2011.
- [22] G. Theocharis, N. Boechler, and C. Daraio. Nonlinear phononic periodic structures and granular crystals. In *Acoustic Metamaterials and Phononic Crystals*, pages 217–251. Springer-Verlag, Berlin, Germany, 2013.
- [23] F. Li, P. Anzel, J. Yang, P.G. Kevrekidis, and C. Daraio. Granular acoustic switches and logic elements. *Nat. Comm.*, 5:5311–5315, 2014.
- [24] Jinkyu Yang, Sophia N. Sangiorgio, Sean L. Borkowski, Claudio Silvestro, Luigi De Nardo, Chiara Daraio, and Edward Ebramzadeh. Site-Specific Quantification of Bone Quality Using Highly Nonlinear Solitary Waves. *Journal of Biomechanical Engineering*, 134(10), 10 2012. 101001.
- [25] H. Hertz. Über die Berührung fester elastischer Körper. *J. Reine. Angew. Math*, 92:156, 1881.
- [26] K. L. Johnson. *Contact Mechanics*. Cambridge University Press, Cambridge, UK, 1985.
- [27] E. Fermi, J. Pasta, and S. Ulam. Studies of Nonlinear Problems. I. *Tech. Rep.*, (Los Alamos National Laboratory, Los Alamos, NM, USA):LA-1940, 1955.

- [28] Mason A. Porter, Norman J. Zabusky, Bambi Hu, and David K. Campbell. Fermi, pasta, ulam and the birth of experimental mathematics: A numerical experiment that enrico fermi, john pasta, and stanislaw ulam reported 54 years ago continues to inspire discovery. *American Scientist*, 97(3):214–221, 2009.
- [29] Thierry Dauxois. Fermi, Pasta, Ulam, and a mysterious lady. *Physics Today*, 61(1):55–57, 01 2008.
- [30] G. Friesecke and R. L. Pego. Solitary waves on Fermi–Pasta–Ulam lattices: I. Linear implies nonlinear stability. *Nonlinearity*, 15:1343, 2002.
- [31] G. Friesecke and R. L. Pego. Solitary waves on Fermi–Pasta–Ulam lattices: III. Howland-type Floquet theory. *Nonlinearity*, 17:207, 2004.
- [32] G. Friesecke and R. L. Pego. Solitary waves on Fermi–Pasta–Ulam lattices: IV. Proof of stability at low energy. *Nonlinearity*, 17:229, 2004.
- [33] Y. Shen, P. G. Kevrekidis, S. Sen, and A. Hoffman. Characterizing traveling-wave collisions in granular chains starting from integrable limits: The case of the Korteweg–de Vries equation and the Toda lattice. *Phys. Rev. E*, 90:022905, 2014.
- [34] Philip Rosenau and James M. Hyman. Compactons: Solitons with finite wavelength. *Phys. Rev. Lett.*, 70:564–567, 1993.
- [35] C. Coste, E. Falcon, and S. Fauve. Solitary waves in a chain of beads under Hertz contact. *Phys. Rev. E*, 56:6104, 1997.
- [36] Karsten Ahnert and Arkady Pikovsky. Compactons and chaos in strongly nonlinear lattices. *Phys. Rev. E*, 79:026209, 2009.
- [37] R. S. MacKay. Solitary waves in a chain of beads under Hertz contact. *Phys. Lett. A*, 251:191, 1999.
- [38] G. Friesecke and J. A. D. Wattis. Existence theorem for solitary waves on lattices. *Commun. Math. Phys.*, 161:391, 1994.
- [39] E. Kim, R. Chaunsali, H. Xu, J. Castillo, J. Yang, P. G. Kevrekidis, and A. F. Vakakis. Nonlinear low-to-high frequency energy cascades in diatomic granular crystals. *Phys. Rev. E*, 92:062201, 2015.
- [40] A. Chatterjee. Asymptotic solution for solitary waves in a chain of elastic spheres. *Phys. Rev. E*, 59:5912, 1999.
- [41] Jared M. English and Robert L. Pego. On the solitary wave pulse in a chain of beads. *Proceedings of the AMS*, 133:1763, 2005.
- [42] D. Hochstrasser, F.G. Mertens, and H. Büttner. An iterative method for the calculation of narrow solitary excitations on atomic chains. *Physica D*, 35:259, 1989.
- [43] K. R. Jayaprakash, Yuli Starosvetsky, and Alexander F. Vakakis. New family of solitary waves in granular dimer chains with no precompression. *Phys. Rev. E*, 83:036606, 2011.

- [44] M. A. Porter, C. Daraio, E. B. Herbold, I. Szelengowicz, and P. G. Kevrekidis. Highly nonlinear solitary waves in periodic dimer granular chains. *Phys. Rev. E*, 77:015601(R), 2008.
- [45] M. A. Porter, C. Daraio, I. Szelengowicz, E. B. Herbold, and P. G. Kevrekidis. Highly nonlinear solitary waves in heterogeneous periodic granular media. *Physica D*, 238:666, 2009.
- [46] K. R. Jayaprakash, Y. Starosvetsky, A. F. Vakakis, and O. V. Gendelman. Nonlinear resonances leading to strong pulse attenuation in granular dimer chains. *J. Nonlinear Sci.*, 23(3):363, 2013.
- [47] K.R. Jayaprakash, A. Shiffer, and Y. Starosvetsky. Traveling waves in trimer granular lattice I: Bifurcation structure of traveling waves in the unit-cell model. *Communications in Nonlinear Science and Numerical Simulation*, 38:8 – 22, 2016.
- [48] K. R. Jayaprakash, Alexander F. Vakakis, and Yuli Starosvetsky. Solitary waves in a general class of granular dimer chains. *J. App. Phys.*, 112(3):034903, 2012.
- [49] Anna Vainchtein, Yuli Starosvetsky, J. Douglas Wright, and Ron Perline. Solitary waves in diatomic chains. *Phys. Rev. E*, 93:042210, Apr 2016.
- [50] T. E. Faver and J. D. Wright. Exact diatomic Fermi–Pasta–Ulam–Tsingou solitary waves with optical band ripples at infinity. *arXiv:1511.00942*, 2015.
- [51] R.K. Dodd, J.C. Eilbeck, J.D. Gibbon, and H.C. Morris. *Solitons and Nonlinear Wave Equations*. Academic Press, San Diego, 1982.
- [52] A. J. Sievers and S. Takeno. Intrinsic localized modes in anharmonic crystals. *Phys. Rev. Lett.*, 61:970–973, Aug 1988.
- [53] J. B. Page. Asymptotic solutions for localized vibrational modes in strongly anharmonic periodic systems. *Phys. Rev. B*, 41:7835–7838, 1990.
- [54] R S MacKay and S Aubry. Proof of existence of breathers for time-reversible or Hamiltonian networks of weakly coupled oscillators. *Nonlinearity*, 7(6):1623, 1994.
- [55] C. Chong, P. G. Kevrekidis, G. Theocharis, and Chiara Daraio. Dark breathers in granular crystals. *Phys. Rev. E*, 87:042202, 2013.
- [56] C. Chong, F. Li, J. Yang, M. O. Williams, I. G. Kevrekidis, P. G. Kevrekidis, and C. Daraio. Damped-driven granular chains: An ideal playground for dark breathers and multibreathers. *Phys. Rev. E*, 89:032924, 2014.
- [57] Guoxiang Huang, Zhu-Pei Shi, and Zaixin Xu. Asymmetric intrinsic localized modes in a homogeneous lattice with cubic and quartic anharmonicity. *Phys. Rev. B*, 47:14561, 1993.
- [58] P. G. Kevrekidis, D. J. Frantzeskakis, and R. Carretero-González. *The Defocusing Nonlinear Schrödinger Equation*. SIAM, Philadelphia, 2015.
- [59] E. Hairer, S.P. Nørsett, and G. Wanner. *Solving Ordinary Differential Equations I*. Springer-Verlag, Berlin, Germany, 1993.

- [60] G. Theocharis, N. Boechler, P. G. Kevrekidis, S. Job, M. A. Porter, and C. Daraio. Intrinsic energy localization through discrete gap breathers in one-dimensional diatomic granular crystals. *Phys. Rev. E*, 82:056604, 2010.
- [61] C. Hoogeboom, Y. Man, N. Boechler, G. Theocharis, P. G. Kevrekidis, I. G. Kevrekidis, and C. Daraio. Hysteresis loops and multi-stability: From periodic orbits to chaotic dynamics (and back) in diatomic granular crystals. *Euro. Phys. Lett.*, 101:44003, 2013.
- [62] S. Flach and A. V. Gorbach. Discrete breathers in Fermi–Pasta–Ulam lattices. *Chaos*, 15:015112, 2005.
- [63] C.C. Chicone. *Ordinary differential equations with applications*. Springer, New York, 1999.
- [64] F. Fraternali, G. Carpentieri, A. Amendola, R. E. Skelton, and V. F. Nesterenko. Multiscale tunability of solitary wave dynamics in tensegrity metamaterials. *Applied Physics Letters*, 105(20):201903, 2014.
- [65] H. Yasuda, C. Chong, E. G. Charalampidis, P. G. Kevrekidis, and J. Yang. Formation of rarefaction waves in origami-based metamaterials. *Phys. Rev. E*, 93:043004, 2016.
- [66] H. Yasuda, Y. Miyazawa, E. G. Charalampidis, C. Chong, P. G. Kevrekidis, and J. Yang. Origami-based impact mitigation via rarefaction solitary wave creation. *Science Advances*, 5:eaau2835, 2019.
- [67] E. B. Herbold and V. F. Nesterenko. Propagation of rarefaction pulses in discrete materials with strain-softening behavior. *Phys. Rev. Lett.*, 110:144101, 2013.
- [68] H. Kim, E. Kim, C. Chong, P. G. Kevrekidis, and J. Yang. Demonstration of dispersive rarefaction shocks in hollow elliptical cylinder chains. *Phys. Rev. Lett.*, 120:194101, 2018.
- [69] G. James, P. G. Kevrekidis, and J. Cuevas. Breathers in oscillator chains with Hertzian interactions. *Physica D*, 251:39, 2013.
- [70] G. Huang and B. Hu. Asymmetric gap soliton modes in diatomic lattices with cubic and quartic nonlinearity. *Phys. Rev. B*, 57:5746, 1998.
- [71] C. Hoogeboom and P.G. Kevrekidis. Breathers in periodic granular chains with multiple band gaps. *Phys. Rev. E*, 86:061305, 2012.
- [72] N. Boechler, G. Theocharis, S. Job, P. G. Kevrekidis, M. A. Porter, and C. Daraio. Discrete breathers in one-dimensional diatomic granular crystals. *Phys. Rev. Lett.*, 104:244302, 2010.
- [73] E. G. Charalampidis, F. Li, C. Chong, J. Yang, and P. G. Kevrekidis. Time-periodic solutions of driven-damped trimer granular crystals. *Math. Probl. in Eng.*, 2015:830978, 2015.
- [74] M. M. Lee, E. G. Charalampidis, S. Xing, C. Chong, and P. G. Kevrekidis. Breathers in lattices with alternating strain-hardening and strain-softening interactions. *Phys. Rev. E*, 107:054208, May 2023.
- [75] G. Theocharis, M. Kavousanakis, P. G. Kevrekidis, C. Daraio, M. A. Porter, and I. G. Kevrekidis. Localized breathing modes in granular crystals with defects. *Phys. Rev. E*, 80:066601, 2009.

- [76] Stéphane Job, Francisco Santibanez, Franco Tapia, and Francisco Melo. Wave localization in strongly nonlinear Hertzian chains with mass defect. *Phys. Rev. E*, 80:025602, Aug 2009.
- [77] Y. Man, N. Boechler, G. Theocharis, P. G. Kevrekidis, and C. Daraio. Defect modes in one-dimensional granular crystals. *Phys. Rev. E*, 85:037601, 2012.
- [78] H.W. Liepmann and A. Roshko. *Elements of Gasdynamics*. Wiley, New York, 1957.
- [79] R. Courant and K. O. Friedrichs. *Supersonic Flow and Shock Waves*. Springer-Verlag, Berlin, 1948.
- [80] J. Smoller. *Shock Waves and Reaction–Diffusion Equations*. Springer-Verlag, New York, 1983.
- [81] D. H. Tsai and C. W. Beckett. Shock wave propagation in cubic lattices. *J. of Geophys. Res.*, 71(10):2601, 1966.
- [82] B. L. Holian. Atomistic computer simulations of shock waves. *Shock Waves*, 5(3):149–157, 1995.
- [83] Jian Li, S Chockalingam, and Tal Cohen. Observation of ultraslow shock waves in a tunable magnetic lattice. *Phys. Rev. Lett.*, 127:014302, Jun 2021.
- [84] Christopher Chong, Ari Geisler, Panayotis Kevrekidis, and Gino Biondini. Integrable approximations of dispersive shock waves of the granular chain. *arXiv:2402.08218*, 2024.
- [85] E. Hascoet and H. J. Herrmann. Shocks in non-loaded bead chains with impurities. *Eur. Phys. J. B*, 14:183, 2000.
- [86] E. B. Herbold and V. F. Nesterenko. Solitary and shock waves in discrete strongly nonlinear double power-law materials. *Appl. Phys. Lett.*, 90(26):261902, 2007.
- [87] A. Molinari and C. Daraio. Stationary shocks in periodic highly nonlinear granular chains. *Phys. Rev. E*, 80:056602, 2009.
- [88] E. B. Herbold and V. F. Nesterenko. Shock wave structure in a strongly nonlinear lattice with viscous dissipation. *Phys. Rev. E*, 75:021304, 2007.
- [89] Shu Jia, Wenjie Wan, and Jason W. Fleischer. Dispersive shock waves in nonlinear arrays. *Phys. Rev. Lett.*, 99:223901, Nov 2007.
- [90] G.B. Whitham. *Linear and Nonlinear Waves*. Wiley, New York, 1974.
- [91] G.A. El, M.A. Hoefer, and M. Shearer. Dispersive and diffusive-dispersive shock waves for nonconvex conservation laws. *SIAM Review*, 59(1):3, 2017.
- [92] M. J. Ablowitz and M. Hoefer. Dispersive shock waves. *Scholarpedia*, 4(11):5562, 2009.
- [93] A. M. Filip and S. Venakides. Existence and modulation of traveling waves in particles chains. *Comm. Pure and Appl. Math.*, 52(6):693, 1999.
- [94] W. Dreyer, M. Herrmann, and A. Mielke. Micro-macro transition in the atomic chain via Whitham’s modulation equation. *Nonlinearity*, 19(2):471, 2005.



- [95] G. A. El. Resolution of a shock in hyperbolic systems modified by weak dispersion. *Chaos: An Interdisciplinary Journal of Nonlinear Science*, 15(3):037103, 10 2005.
- [96] Patrick Sprenger, Christopher Chong, Emmanuel Okyere, Michael Herrmann, Panayotis Kevrekidis, and Mark Hoefer. Dispersive hydrodynamics of a discrete conservation law. *arXiv:2404.1675*, 2024.
- [97] Christopher Chong, Michael Herrmann, and P.G. Kevrekidis. Dispersive shock waves in lattices: A dimension reduction approach. *Physica D: Nonlinear Phenomena*, 442:133533, 2022.
- [98] F.W. Olver, D.W. Lozier, R.F. Boisvert, and C.W. Clark. *NIST Handbook of Mathematical Functions*. Cambridge University Press, 2010.
- [99] A. V. Gurevich and L. P. Pitaevskii. Nonstationary structure of a collisionless shock wave. *Zhurnal Eksperimentalnoi i Teoreticheskoi Fiziki*, 65:590–604, 1973.
- [100] A M Kamchatnov. *Nonlinear Periodic Waves and Their Modulations*. World Scientific, 2000.
- [101] Yuji Kodama. The whitham equations for optical communications: Mathematical theory of nrz. *SIAM Journal on Applied Mathematics*, 59(6):2162–2192, 1999.
- [102] Mielke Alexander and Patz Carsten. Uniform asymptotic expansions for the fundamental solution of infinite harmonic chains. *Z. Anal. Anwend.*, 36:437–475, 2017.
- [103] A. M. Bloch and Y. Kodama. Dispersive regularization of the whitham equation for the toda lattice. *SIAM Journal on Applied Mathematics*, 52(4):909–928, 1992.
- [104] Gino Biondini, Christopher Chong, and Panayotis Kevrekidis. On the whitham modulation equations for the toda lattice and the quantitative characterization of its dispersive shocks. *ArXiv:2312.10755*, 2023.
- [105] P. Rosenau. Dynamics of nonlinear mass-spring chains near the continuum limit. *Phys. Lett. A*, 118:222, 1986.
- [106] P. Rosenau. Hamiltonian dynamics of dense chains and lattices: Or how to correct the continuum. *Phys. Lett. A*, 311:39, 2003.
- [107] S. Yang, G. Biondini, C. Chong, and P. G. Kevrekidis. Dispersive shock waves in granular crystals without precompression. *in preparation*, 2024.
- [108] Alejandro J. Martínez, P. G. Kevrekidis, and Mason A. Porter. Superdiffusive transport and energy localization in disordered granular crystals. *Phys. Rev. E*, 93:022902, Feb 2016.
- [109] E. Kim, A. Martínez, S. Phenisee, P. G. Kevrekidis, M. A. Porter, and J. Yang. Direct measurement of superdiffusive energy transport and energy localization in disordered granular chains. *Nature Communications*, 9:640, 2018.
- [110] G. James, P. G. Kevrekidis, and J. Cuevas. Breathers in oscillator chains with hertzian interactions. *Physica D: Nonlinear Phenomena*, 251:39–59, 2013.
- [111] Lifeng Liu, Guillaume James, Panayotis Kevrekidis, and Anna Vainchtein. Strongly nonlinear waves in locally resonant granular chains. *Nonlinearity*, 29(11):3496, 2016.

- [112] L. Liu, G. James, P. G. Kevrekidis, and A. Vainchtein. Breathers in a locally resonant granular chain with precompression. *arXiv:1603.06033*, 2016.
- [113] Timothy E. Faver and Hermen Jan Hupkes. Micropterons, nanopterons and solitary wave solutions to the diatomic fermi–pasta–ulam–tsingou problem. *Partial Differential Equations in Applied Mathematics*, 4:100128, 2021.
- [114] K. Vorotnikov, Y. Starosvetsky, G. Theocharis, and P.G. Kevrekidis. Wave propagation in a strongly nonlinear locally resonant granular crystal. *Physica D: Nonlinear Phenomena*, 365:27–41, 2018.
- [115] H. Xu, P. G. Kevrekidis, and A. Stefanov. Traveling waves and their tails in locally resonant granular systems. *J. Phys. A: Math. Theor.*, 48:195204, 2015.
- [116] E. Kim, F. Li, C. Chong, G. Theocharis, J. Yang, and P. G. Kevrekidis. Highly nonlinear wave propagation in elastic woodpile periodic structures. *Phys. Rev. Lett.*, 114:118002, 2015.
- [117] Anna Vainchtein. Solitary waves in FPU-type lattices. *Physica D: Nonlinear Phenomena*, 434:133252, 2022.
- [118] M. Molerón, A. Leonard, and C. Daraio. Solitary waves in a chain of repelling magnets. *Journal of Applied Physics*, 115(18):184901, 2014.
- [119] M. Molerón, C. Chong, A. J. Martínez, M. A. Porter, P. G. Kevrekidis, and C. Daraio. Non-linear excitations in magnetic lattices with long-range interactions. *New Journal of Physics*, 21:063032, 2019.
- [120] C. Chong, Y. Wang, D. Marechal, E. G. Charalampidis, Miguel Molerón, Alejandro J. Martínez, Mason A. Porter, P. G. Kevrekidis, and Chiara Daraio. Nonlinear localized modes in two-dimensional hexagonally-packed magnetic lattices. *New Journal of Physics*, 23:043008, 2021.
- [121] B. L. Kim, C. Chong, S. Hajarolasvadi, Y. Wang, and C. Daraio. Dynamics of time-modulated, nonlinear phononic lattices. *Phys. Rev. E*, 107:034211, Mar 2023.
- [122] Christopher Chong, Brian Kim, Evelyn Wallace, and Chiara Daraio. Modulation instability and wavenumber bandgap breathers in a time layered phononic lattice. *Phys. Rev. Res.*, 6:023045, Apr 2024.
- [123] S. Flach. Breathers on lattices with long range interaction. *Phys. Rev. E*, 58:R4116–R4119, Oct 1998.
- [124] P.G. Kevrekidis and J. Cuevas. *Fractional Dispersive Models and Applications*. Springer-Verlag, Heidelberg, 2024.
- [125] Mario I. Molina. Fractional nonlinear electrical lattice. *Phys. Rev. E*, 104:024219, Aug 2021.
- [126] T Bountis J E Macias Diaz. An efficient dissipation-preserving numerical scheme to solve a caputo–riesz time-space-fractional nonlinear wave equation. *Fractal/Fractional*, 6(9):500–525, 2022.
- [127] Tomoki Ozawa, Hannah M. Price, Alberto Amo, Nathan Goldman, Mohammad Hafezi, Ling Lu, Mikael C. Rechtsman, David Schuster, Jonathan Simon, Oded Zilberberg, and Iacopo Carusotto. Topological photonics. *Rev. Mod. Phys.*, 91:015006, Mar 2019.

- [128] Zhihao Lan, Menglin L.N. Chen, Fei Gao, Shuang Zhang, and Wei E.I. Sha. A brief review of topological photonics in one, two, and three dimensions. *Reviews in Physics*, 9:100076, 2022.
- [129] Xiang Ni, Simon Yves, Alex Krasnok, and Andrea Alu. Topological metamaterials. *Chemical Reviews*, 123(12):7585–7654, 2023.
- [130] Xiujuan Zhang, Meng Xiao, Ying Cheng, Ming-Hui Lu, and Johan Christensen. Topological sound. *Communications Physics*, 1(1):97, 2018.
- [131] Haoran Xue, Yihao Yang, and Baile Zhang. Topological acoustics. *Nature Reviews Materials*, 7(12):974–990, 2022.
- [132] Li Xin, Yu Siyuan, Liu Harry, Lu Minghui, and Chen Yanfeng. Topological mechanical metamaterials: A brief review. *Current Opinion in Solid State and Materials Science*, 24(5):100853, 2020.
- [133] Mark J. Ablowitz and Justin T. Cole. Nonlinear optical waveguide lattices: Asymptotic analysis, solitons, and topological insulators. *Physica D: Nonlinear Phenomena*, 440:133440, 2022.
- [134] Daniel Leykam, Sergej Flach, Omri Bahat-Treidel, and Anton S. Desyatnikov. Flat band states: Disorder and nonlinearity. *Phys. Rev. B*, 88:224203, December 2013.
- [135] Daniel Leykam, Alexei Andreanov, and Sergej Flach. Artificial flat band systems: from lattice models to experiments. *Adv. Phys.: X*, 3(1):1473052, 2018.
- [136] Pragalv Karki and Jayson Paulose. Non-singular and singular flat bands in tunable phononic metamaterials. *Phys. Rev. Res.*, 5:023036, Apr 2023.
- [137] Ya-Xi Shen, Yu-Gui Peng, Pei-Chao Cao, Jensen Li, and Xue-Feng Zhu. Observing localization and delocalization of the flat-band states in an acoustic cubic lattice. *Phys. Rev. B*, 105:104102, Mar 2022.
- [138] Carys Chase-Mayoral, L. Q. English, Noah Lape, Yeongjun Kim, Sanghoon Lee, Alexei Andreanov, Sergej Flach, and P. G. Kevrekidis. Compact localized states in electric circuit flat-band lattices. *Phys. Rev. B*, 109:075430, Feb 2024.
- [139] Rodrigo A. Vicencio and Magnus Johansson. Discrete flat-band solitons in the kagome lattice. *Phys. Rev. A*, 87:061803, Jun 2013.
- [140] Seababrata Mukherjee, Alexander Spracklen, Debaditya Choudhury, Nathan Goldman, Patrik Öhberg, Erika Andersson, and Robert R. Thomson. Observation of a localized flat-band state in a photonic lieb lattice. *Phys. Rev. Lett.*, 114:245504, Jun 2015.
- [141] Rodrigo A. Vicencio, Camilo Cantillano, Luis Morales-Inostroza, Bastián Real, Cristian Mejía-Cortés, Steffen Weimann, Alexander Szameit, and Mario I. Molina. Observation of localized states in Lieb photonic lattices. *Phys. Rev. Lett.*, 114:245503, June 2015.
- [142] Luis Morales-Inostroza and Rodrigo A. Vicencio. Simple method to construct flat-band lattices. *Phys. Rev. A*, 94:043831, October 2016.
- [143] A. Leonard, C. Chong, P. G. Kevrekidis, and C. Daraio. Traveling waves in 2D hexagonal granular crystal lattices. *Granular Matter*, 16(4):531, 2014.

- [144] Raj Kumar Pal, Javier Vila, Michael Leamy, and Massimo Ruzzene. Amplitude-dependent topological edge states in nonlinear phononic lattices. *Phys. Rev. E*, 97:032209, Mar 2018.
- [145] Shuaifeng Li, Panayotis G. Kevrekidis, and Jinkyu Yang. Characterization of elastic topological states using dynamic mode decomposition. *Phys. Rev. B*, 107:184308, May 2023.
- [146] Joshua R. Tempelman, Alexander F. Vakakis, and Kathryn H. Matlack. A modal decomposition approach to topological wave propagation. *Journal of Sound and Vibration*, 568:118033, 2024.
- [147] Matthew J. Colbrook. The multiverse of dynamic mode decomposition algorithms, 2023.
- [148] Guillaume James. Traveling fronts in dissipative granular chains and nonlinear lattices. *Nonlinearity*, 34(3):1758, mar 2021.
- [149] M. Raissi, P. Perdikaris, and G. E. Karniadakis. Physics-informed neural networks: A deep learning framework for solving forward and inverse problems involving nonlinear partial differential equations. *Journal of Computational Physics*, 378:686–707, February 2019.
- [150] S.L. Brunton, J.L. Proctor, and J.N. Kutz. Discovering governing equations from data by sparse identification of nonlinear dynamical systems. *Proceedings of the National Academy of Sciences*, 113(15):3932–3937, April 2016.
- [151] L. Lu, X. Meng, Z. Mao, and G.E. Karniadakis. DeepXDE: A deep learning library for solving differential equations. *SIAM Review*, 63(1):208–228, 2021.
- [152] G.E. Karniadakis, I.G. Kevrekidis, L. Lu, P. Perdikaris, S. Wang, and L. Yang. Physics-informed machine learning. *Nature Reviews Physics*, 3(6):422–440, 2021.
- [153] Sheikh Saqlain, Wei Zhu, Efstathios G. Charalampidis, and Panayotis G. Kevrekidis. Discovering governing equations in discrete systems using pinns. *Communications in Nonlinear Science and Numerical Simulation*, 126:107498, 2023.